Bimetallic Nanoparticles

DOI: 10.1002/anie.201207824

Gold–Palladium Core–Shell Nanocrystals with Size and Shape Control Optimized for Catalytic Performance**

*Anna M. Henning, John Watt, Peter J. Miedziak, Soshan Cheong, Marco Santonastaso, Minghui Song, Yoshihiko Takeda, Angus I. Kirkland, Stuart H. Taylor, and Richard D. Tilley**

Bimetallic nanocrystals are a promising new class of materials to meet increasing industrial demand for optimized catalysts. Owing to synergistic effects between two metals, bimetallic nanocrystalline catalysts often display superior catalytic performance compared to their single metal counterparts.[1] As the composition of core–shell nanocrystals can be precisely tuned through control of the shell thickness, the catalytic activity of these systems can be readily optimized.[2] Close control over nanocrystal size and shape is also essential for controlling catalytic properties.[3] Herein we report the synthesis of small (<15 nm), monodispersed uniform icosahedral Au–Pd core–shell nanocrystals, with a range of shell thicknesses. The critical step in our synthesis is an extremely slow growth rate, which allows precise tuning of the palladium shell thickness, while maintaining a highly faceted icosahedral shape. We show that the catalytic properties of the Au–Pd core–shell nanocrystals can be optimized for the oxidation of benzyl alcohol to benzaldehyde, an important industrial product.

Bimetallic core–shell nanocrystals are key candidates for future heterogeneous catalysis, as unlike many doped or alloyed nanostructures, all surface atoms can be tailored to be the desired catalytically active metal. To date, previous synthetic investigations have resulted in a variety of faceted shapes of larger sized (ca. 20–200 nm) bimetallic nanocrystals.[4] However, faceted particles less than 15 nm in size have maximized catalytic performance and have proved challenging to synthesize.[1a,3a–d] Of the many possible bimetallic systems, gold–palladium is one of the most exciting for catalytic studies,[1b,c] as gold–palladium catalysts are important for the direct formation of hydrogen peroxide,[5] vinyl acetate synthesis,[1b,3a] carbon monoxide oxidation,[1b,3a,6] and the oxidation of primary alcohols,[1a,7] all of which are key reactions in the petrochemical and pharmaceutical industries.

Our strategy for synthesizing highly faceted icosahedral Au–Pd core–shell nanocrystals is by using a seed-mediated approach, which enables the independent control of nucleation and growth stages.[8] Initially, highly faceted, monodisperse icosahedral gold nanocrystal seeds (7.1 ± 0.4 nm in size) were synthesized (Supporting Information, Figure S1). To grow the palladium shell, the gold seed solution was added to a precursor solution containing palladium acetylacetonate and hexadecylamine in toluene, in a 2:1 molar ratio of palladium to gold; this reaction mixture was then reduced under hydrogen at 60 °C for 120 min.

The key step in our synthesis is the layer by layer atomic addition of Pd^0 to the surface of the gold nanocrystal seeds, thus enabling slow, controlled growth of the palladium shell with time. This growth regime means that it is simple to quench the growth at different reaction times to give finely controlled palladium shell thicknesses. Most importantly, the icosahedral morphology of the seed is maintained during the slow growth.

A transmission electron microscopy (TEM) image of the Au–Pd core–shell nanocrystals is shown in Figure 1a. The nanocrystals are 11.4 ± 0.4 nm in size and monodisperse with well-defined faceting, and form a honeycomb-like monolayer when deposited on a TEM grid. A high resolution TEM image of a single Au–Pd core–shell nanocrystal is shown in Figure 1b. The atomic lattice fringes are continuous from the center of the nanocrystal to the edge, thus indicating epitaxial growth of palladium onto the gold seeds. Epitaxial growth is expected as the lattice mismatch between gold and palladium is less than 5 %.[4a] The TEM image corresponds to a multiply

[*] A. M. Henning, Dr. J. Watt, Prof. R. D. Tilley
School of Chemical and Physical Sciences and the MacDiarmid Institute for Advanced Materials and Nanotechnology
Victoria University of Wellington
Kelburn Parade, Wellington 6012 (New Zealand)
E-mail: richard.tilley@vuw.ac.nz

Dr. P. J. Miedziak, M. Santonastaso, Dr. S. H. Taylor
School of Chemistry and Cardiff Catalysis Institute
Cardiff University, Park Place, Cardiff CF10 3AT (UK)

Dr. S. Cheong
Industrial Research Limited and the MacDiarmid Institute for Advanced Materials and Nanotechnology
69 Gracefield Road, Lower Hutt 5040 (New Zealand)

Dr. M. Song
Surface Physics and Structure Unit
Advanced Key Technologies Division
National Institute for Materials Science
Sengen 1-2-1, Tsukuba, Ibaraki 305-0047 (Japan)

Dr. Y. Takeda
Quantum Beam Unit, Advanced Key Technologies Division
National Institute for Materials Science
3-13 Sakura, Ibaraki 305-0003, Tsukuba (Japan)

Prof. A. I. Kirkland
Department of Materials, University of Oxford
Parks Road, Oxford OX1 3PH (UK)

[**] R.D.T., J.W., and S.C. thank the MacDiarmid Institute and MSI for funding through grants PROJ-13733-NMTS, CONT-21040-IIOF-VICKLINK, and CONT-20707-NMTS-IRL. Funding from EPSRC (Grant EP/F048009/1) is acknowledged together with technical support from JEOL Ltd.

Supporting information for this article is available on the WWW under http://dx.doi.org/10.1002/anie.201207824.

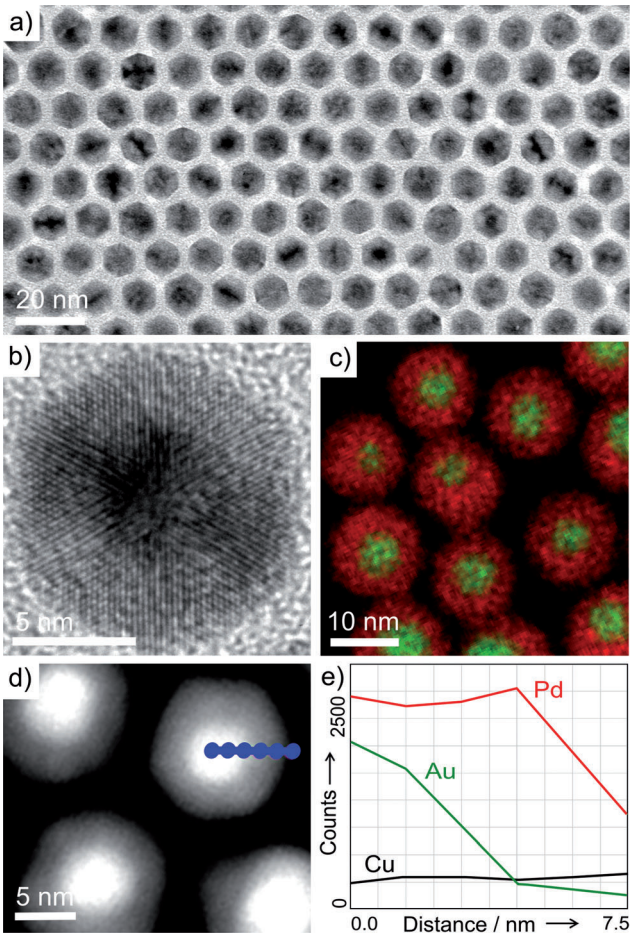

Figure 1. a) Bright-field TEM image of an array of 11.4 nm highly faceted Au–Pd core–shell nanocrystals. b) High-resolution TEM image of a single Au–Pd core–shell nanocrystal, with a clear contrast difference between the dark core (gold) and lighter shell (palladium). Lattice fringes correspond to an icosahedral structure oriented along ⟨111⟩. c) STEM-EDX map shown as an overlay of gold and palladium signals, confirming the core–shell structure. d) HAADF-STEM image showing a contrast difference between gold core (bright) and palladium shell (dark). Dotted blue line represents the EDX line scan shown in e) with palladium in red, gold in green and copper in black.

twinned icosahedral morphology viewed along a ⟨111⟩ zone axis, with only {111} surfaces exposed.[9]

The nanocrystals were also analysed using Scanning TEM (STEM) coupled with energy dispersive X-ray spectroscopy (EDX) to confirm the composition of the bimetallic particles. An overlay of palladium and gold EDX maps is shown in Figure 1 c (and Supporting Information, Figure S2), indicating a clear separation of the two elements and confirming the core–shell structure. The high-angle annular dark-field (HAADF) STEM image in Figure 1 d also shows a clear contrast difference between the gold core and palladium shell. An EDX line from a single nanocrystal from the image in Figure 1 d is shown by a dotted blue line, with the resultant compositional profile shown in Figure 1 e; this compositional profile is consistent with a polyhedral core–shell particle, in which the gold count decreases from the center of the particle with respect to palladium. Finally UV-Vis spectroscopy was used to confirm the absence of uncoated gold cores in the sample (Supporting Information, Figure S3).

Time-resolved experiments were performed to investigate how faceting is maintained at a small particle size and to synthesize nanocrystals with different shell thicknesses for subsequent catalytic studies. Samples of nanocrystals were isolated by quenching the reaction at 30, 60, 90, 120, and 180 min and size distributions measured from TEM images (Supporting Information, Figure S4 and S5). From measurements of the increase in the mean size of the nanocrystals, the change in palladium shell thickness as a function of reaction time was calculated, giving shell thicknesses of 0.4, 0.8, 1.5, 2.2, and 3.2 nm after 30, 60, 90, 120, and 180 min, respectively. The gold cores appear to maintain a constant size over the course of the reaction. A thin alloy region between the core and the shell cannot be discounted because of local variations in particle orientation and from the resolution of the images, which make such alloying hard to observe.

The measured palladium shell thicknesses were plotted against reaction time (Figure 2) and the rate of palladium shell growth calculated as 1 atomic layer of palladium

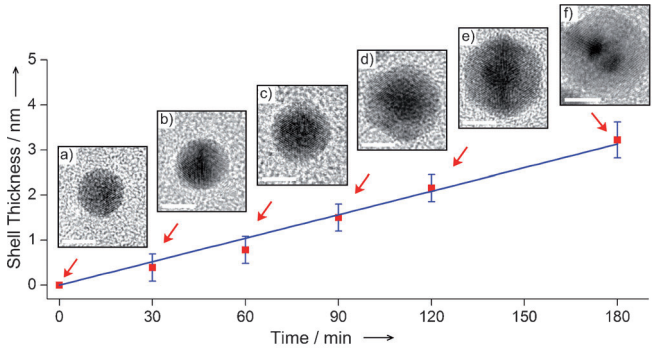

Figure 2. Palladium shell thickness (nm) versus time (min) for the growth of faceted icosahedral Au–Pd core–shell nanocrystals. Time-resolved samples were obtained by quenching the reaction at 30, 60, 90, 120, and 180 min. The size distributions of each sample were measured and the shell thickness was calculated by subtracting the size of the gold seed. Standard size deviation is shown as error bars. Representative HRTEM images of each sample are shown in a)–f). Scale bars: 5 nm.

deposited every 13 min. This growth rate is extremely slow compared to previously reported syntheses. For example, calculations from the data of the groups of Wiley and Xia show a growth rate of 1 atomic layer every 2 min for the seed-mediated growth of Au–Pd nanodendrites,[10] and a growth rate of 1 atomic layer every 4.5 min for the synthesis of 12–38 nm Au–Pd nanocubes.[11] Figure 3 shows that there is linear growth of the palladium shell over the course of the entire reaction. This type of growth has previously been shown to produce thermodynamically stable nanocrystal shapes for palladium,[12] thus implying that growth of our Au–Pd core–shell nanocrystals is thermodynamically controlled.

In thermodynamically controlled growth, palladium atoms have sufficient time post deposition to migrate to the lowest energy surface site, thus maintaining the initial

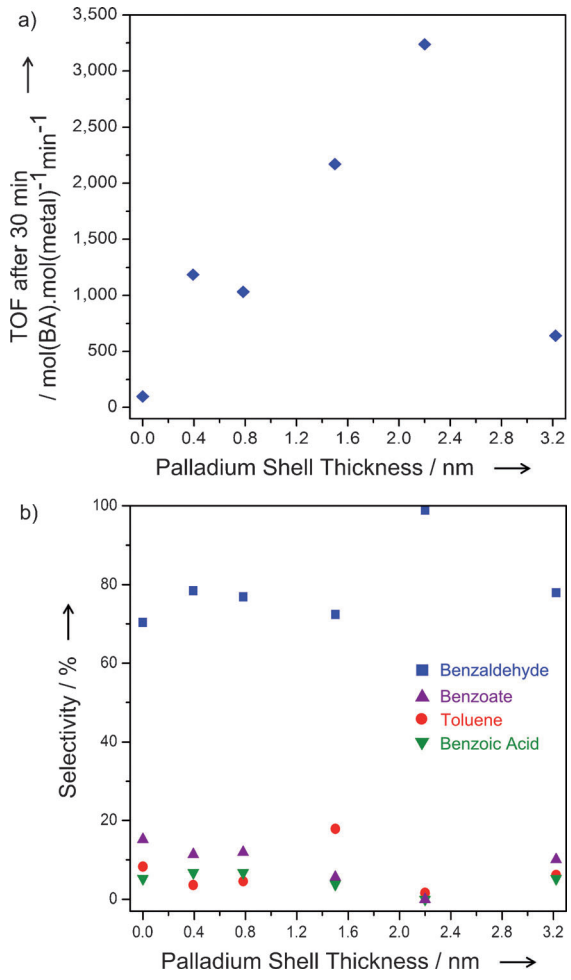

Figure 3. Catalytic properties of icosahedral Au–Pd core–shell nanocrystals with varying palladium shell thicknesses for the solvent-free oxidation of benzyl alcohol. a) Turnover frequency (TOF) versus palladium shell thickness. b) Selectivity to products in the oxidation of benzyl alcohol versus palladium shell thickness.

icosahedral morphology with {111} surface facets.[13] The persistence of an icosahedral morphology was confirmed from HRTEM images of nanocrystals sampled from each reaction (Figure 2a–f). These each show multiply twinned icosahedra oriented along a ⟨111⟩ zone axis, thus indicating the Au–Pd core–shell nanocrystals maintain their faceted icosahedral shape throughout the growth process.

These Au–Pd core–shell systems can be designed and optimized to achieve nanocrystals with maximum catalytic performance, as the bimetallic composition can be finely tuned by controlling the thickness of the shell formed around a uniform core, while a faceted and thermodynamically stable morphology is maintained. To demonstrate the catalytic performance, a series of nanocrystals were used as catalysts for the oxidation of benzyl alcohol to benzaldehyde, which is an important probe reaction and an important industrial step in the oxidation pathway of toluene derivatives.[1a,7]

The nanocrystals studied were taken from the entire range of time resolved experiments shown in Figure 3 with average palladium shell thicknesses of 0.4, 0.8, 1.5, 2.2, and 3.2 nm. In addition, 7.1 nm pure gold cores were studied as a control. All catalysts were prepared with a loading of 1 wt% metal nanoparticles on activated carbon. Solvent-free benzyl alcohol (40 mL) was converted into benzaldehyde in an autoclave under 10 bar oxygen at 140 °C in the presence of 25 mg of the Au-Pd/C catalyst (see the Supporting Information for experimental details).

The data shown in Figure 3 clearly show peaks in the catalytic performance, measured as both turnover frequency (TOF) and selectivity, for nanocrystals with a shell thickness of 2.2 nm (ca. 12 atomic layers of palladium). The maximum activity occurs at a shell thickness of 2.2 nm (Figure 3a) when the bimetallic synergy between gold and palladium is optimized; thinner or thicker shells become more gold- or palladium-like, thus resulting in lower activities.[1a] A maximum selectivity of greater than 95% for benzaldehyde is also achieved for a shell thickness of 2.2 nm (Figure 3b). Moreover, the consistently high selectivity (greater than 70%) for all shell thicknesses indicates that maintaining a faceted morphology leads to good catalytic selectivity over a range of compositions. We also note that as the shell thickness increases from 1.5 nm to 2 nm, the faceting of the particles becomes more pronounced; this more-pronounced faceting may also contribute to the increases in TOF and in selectivity observed. Further catalytic characterization is given in the Supporting Information (Figure S6).

In summary, we have described a method for the synthesis of highly faceted, icosahedral Au–Pd core–shell nanocrystals, far smaller than any previously produced. The control of the size and shape is achieved by the extremely slow growth of the palladium shell on the gold core, thus enabling precise, layer by layer, control of the shell thickness. The catalytic properties of the Au–Pd core–shell nanocrystals for the industrially important oxidation of benzyl alcohol have been tested and the shell thickness of the nanocrystals that give maximum catalytic performance can be identified and these nanocrystals can be isolated. This concept of extremely slow shell growth unlocks the possibility for future nanocrystal catalyst design where all three critical variables of size, shape and composition can be optimized for a given catalytic reaction.

Experimental Section

Synthesis of gold seeds: Gold chloride trihydrate (19.7 mg, Aldrich, 99.9%) was dissolved in toluene (1 mL; > 99% HPLC grade) along with dodecylamine (0.185 g; 0.1 mmol; Aldrich, 98%) in a 11 mL sample vial. The vial was placed in a 10 oz. Fischer-Porter bottle filled with 10 mL of excess toluene and sealed with bivalves. Air was evacuated from the bottle and then repeatedly purged with vacuum and hydrogen gas (1 bar). The bottle was then filled with hydrogen gas (3 bar) and placed in an oven at 60 °C for 24 h. The gas was released, the solution washed once with an equal amount of methanol in a macrocentrifuge for 15 min at 4000 rpm, and then the product was stored as a powder.

Typical synthesis of Au–Pd core–shell nanoparticles: Hexadecylamine (0.12 g; Aldrich, 90%) was added, as surfactant, to a solution of palladium acetylacetonate ([Pd(acac)$_2$]; 15.2 mg; Aldrich, 99%) in toluene in a sample vial. The gold seeds prepared as above were added to the reaction mixture to give a Pd/Au molar ratio of 2:1, and a total solvent volume of 1 mL. The vial was placed in a 10 oz. Fischer-Porter bottle and prepared as described above. The bottle was then filled with 1 bar of hydrogen gas and placed in an oven at 60 °C for 2 h.

The solution was then removed and the product washed twice by centrifugation at 14000 rpm using an equal amount of methanol.

Characterization: Low- and high-resolution TEM images were recorded using a JEOL 2010 electron microscope operated at 200 kV. Scanning TEM images were recorded using a JEOL 2100F Field Emission microscope. EDX maps were recorded using a JEOL 2800 Field Emission emicroscope fitted with a Centurio 100 mm2 SDD EDX detector giving a solid angle of 0.95 sr. EDX maps were acquired with a probe size of 1 nm and a probe current of 1nA. In all cases TEM samples were prepared by redispersing the dried samples in toluene and dropping the liquid sample onto carbon-coated copper grids.

Received: September 28, 2012
Published online: December 13, 2012

Keywords: bimetallic nanoparticles · core–shell structures · gold · heterogeneous catalysis · palladium

[1] a) D. I. Enache, J. K. Edwards, P. Landon, B. Solsona-Espriu, A. F. Carley, A. A. Herzing, M. Watanabe, C. J. Kiely, D. W. Knight, G. J. Hutchings, *Science* **2006**, *311*, 362; b) T. T. David, *Platinum Met. Rev.* **2004**, *48*, 169; c) C. Mingshu, K. Dheeraj, Y. Cheol-Woo, D. W. Goodman, *Science* **2005**, *310*, 291; d) L. Guczi, *Catal. Today* **2005**, *101*, 53.

[2] a) P. Strasser, S. Koh, T. Anniyev, J. Greeley, K. More, C. F. Yu, Z. C. Liu, S. Kaya, D. Nordlund, H. Ogasawara, M. F. Toney, A. Nilsson, *Nat. Chem.* **2010**, *2*, 454; b) K. Tedsree, T. Li, S. Jones, C. W. A. Chan, K. M. K. Yu, P. A. J. Bagot, E. A. Marquis, G. D. W. Smith, S. C. E. Tsang, *Nat. Nanotechnol.* **2011**, *6*, 302; c) F. Wang, L. D. Sun, W. Feng, H. J. Chen, M. H. Yeung, J. F. Wang, C. H. Yan, *Small* **2010**, *6*, 2566; d) S. Alayoglu, A. U. Nilekar, M. Mavrikakis, B. Eichhorn, *Nat. Mater.* **2008**, *7*, 333; e) Y. Ma, W. Li, E. C. Cho, Z. Li, T. Yu, J. Zeng, Z. Xie, Y. Xia, *ACS Nano* **2010**, *4*, 6725; f) L. Wang, Y. Yamauchi, *J. Am. Chem. Soc.* **2010**, *132*, 13636; g) C. J. Serpell, J. Cookson, D. Ozkaya, P. D. Beer, *Nat. Chem.* **2011**, *3*, 478.

[3] a) G. J. Hutchings, M. Haruta, *Appl. Catal. A* **2005**, *291*, 2; b) A. T. Bell, *Science* **2003**, *299*, 1688; c) M. H. Shao, A. Peles, K. Shoemaker, *Nano Lett.* **2011**, *11*, 3714; d) M. Crespo-Quesada, A. Yarulin, M. S. Jin, Y. N. Xia, L. Kiwi-Minsker, *J. Am. Chem. Soc.* **2011**, *133*, 12787; e) I. Lee, F. Delbecq, R. Morales, M. A. Albiter, F. Zaera, *Nat. Mater.* **2009**, *8*, 132; f) K. M. Bratlie, H. Lee, K. Komvopoulos, P. D. Yang, G. A. Somorjai, *Nano Lett.* **2007**, *7*, 3097; g) J. Zhang, H. Z. Yang, J. Y. Fang, S. Z. Zou, *Nano Lett.* **2010**, *10*, 638.

[4] a) F. R. Fan, D. Y. Liu, Y. F. Wu, S. Duan, Z. X. Xie, Z. Y. Jiang, Z. Q. Tian, *J. Am. Chem. Soc.* **2008**, *130*, 6949; b) C. W. Yang, K. Chanda, P. H. Lin, Y. N. Wang, C. W. Liao, M. H. Huang, *J. Am. Chem. Soc.* **2011**, *133*, 19993; c) C. L. Lu, K. S. Prasad, H. L. Wu, J. A. A. Ho, M. H. Huang, *J. Am. Chem. Soc.* **2010**, *132*, 14546; d) S. E. Habas, H. Lee, V. Radmilovic, G. A. Somorjai, P. Yang, *Nat. Mater.* **2007**, *6*, 692; e) A. N. Wang, Q. Peng, Y. D. Li, *Chem. Mater.* **2011**, *23*, 3217; f) D. Kim, Y. W. Lee, S. B. Lee, S. W. Han, *Angew. Chem.* **2012**, *124*, 163; *Angew. Chem. Int. Ed.* **2012**, *51*, 159; g) C. J. DeSantis, A. A. Peverly, D. G. Peters, S. E. Skrabalak, *Nano Lett.* **2011**, *11*, 2164.

[5] a) J. K. Edwards, A. F. Carley, A. A. Herzing, C. J. Kiely, G. J. Hutchings, *Faraday Discuss.* **2008**, *138*, 225; b) J. K. Edwards, B. E. Solsona, P. Landon, A. F. Carley, A. Herzing, C. J. Kiely, G. J. Hutchings, *J. Catal.* **2005**, *236*, 69.

[6] J. Xu, T. White, P. Li, C. H. He, J. G. Yu, W. K. Yuan, Y. F. Han, *J. Am. Chem. Soc.* **2010**, *132*, 10398.

[7] P. J. Miedziak, Q. He, J. K. Edwards, S. H. Taylor, D. W. Knight, B. Tarbit, C. J. Kiely, G. J. Hutchings, *Catal. Today* **2011**, *163*, 47.

[8] Y. Xia, Y. J. Xiong, B. Lim, S. E. Skrabalak, *Angew. Chem.* **2009**, *121*, 62; *Angew. Chem. Int. Ed.* **2009**, *48*, 60.

[9] a) A. I. Kirkland, D. A. Jefferson, D. Tang, P. P. Edwards, *Proc. R. Soc. London Ser. A* **1991**, *434*, 279; b) J. Reyes-Gasga, S. Tehuacanero-Nunez, J. M. Montejano-Carrizales, X. X. Gao, M. Jose-Yacaman, *Top. Catal.* **2007**, *46*, 23.

[10] J. G. Xu, A. R. Wilson, A. R. Rathmell, J. Howe, M. F. Chi, B. J. Wiley, *ACS Nano* **2011**, *5*, 6119.

[11] J. Li, Y. Zheng, J. Zeng, Y. Xia, *Chem. Eur. J.* **2012**, *18*, 8150.

[12] J. Watt, S. Cheong, M. F. Toney, B. Ingham, J. Cookson, P. T. Bishop, R. D. Tilley, *ACS Nano* **2010**, *4*, 396.

[13] a) A. Howie, L. D. Marks, *Philos. Mag.* **1984**, *49*, 95; b) F. Baletto, R. Ferrando, *Rev. Mod. Phys.* **2005**, *77*, 371.

